LETTER

doi:10.1038/nature25791

Possible interaction between baryons and dark-matter particles revealed by the first stars

Rennan Barkana[1]

The cosmic radio-frequency spectrum is expected to show a strong absorption signal corresponding to the 21-centimetre-wavelength transition of atomic hydrogen around redshift 20, which arises from Lyman-α radiation from some of the earliest stars[1–4]. By observing this 21-centimetre signal—either its sky-averaged spectrum[5] or maps of its fluctuations, obtained using radio interferometers[6,7]—we can obtain information about cosmic dawn, the era when the first astrophysical sources of light were formed. The recent detection of the global 21-centimetre spectrum[5] reveals a stronger absorption than the maximum predicted by existing models, at a confidence level of 3.8 standard deviations. Here we report that this absorption can be explained by the combination of radiation from the first stars and excess cooling of the cosmic gas induced by its interaction with dark matter[8–10]. Our analysis indicates that the spatial fluctuations of the 21-centimetre signal at cosmic dawn could be an order of magnitude larger than previously expected and that the dark-matter particle is no heavier than several proton masses, well below the commonly predicted mass of weakly interacting massive particles. Our analysis also confirms that dark matter is highly non-relativistic and at least moderately cold, and primordial velocities predicted by models of warm dark matter are potentially detectable. These results indicate that 21-centimetre cosmology can be used as a dark-matter probe.

An excess 21-cm absorption signal is a clear sign of scattering of baryons and dark-matter particles. In general, the intensity of the 21-cm signal is expressed as the observed brightness temperature relative to the cosmic microwave background (CMB), which is given by[1]

$$T_{21}=26.8x_{\rm HI}\frac{\rho_{\rm g}}{\overline{\rho}_{\rm g}}\left(\frac{\Omega_{\rm b}h}{0.0327}\right)\left(\frac{\Omega_{\rm m}}{0.307}\right)^{-1/2}\left(\frac{1+z}{10}\right)^{1/2}\left(\frac{T_{\rm S}-T_{\rm CMB}}{T_{\rm S}}\right) \quad (1)$$

in millikelvin. In equation (1), $x_{\rm HI}$ is the mass fraction of neutral (that is, not ionized) hydrogen; $\rho_{\rm g}$ is the gas density and $\overline{\rho}_{\rm g}$ is its cosmic mean value; $\Omega_{\rm m}$ and $\Omega_{\rm b}$ are the cosmic mean densities of matter and baryons, respectively, in units of the critical density (the mean density of a flat universe); h is the Hubble parameter in units of 100 km s^{-1} Mpc^{-1}; z is the redshift that corresponds to an observed wavelength of $21(1+z)$ cm and an observed frequency of $1{,}420/(1+z)$ MHz; $T_{\rm CMB}=2.725(1+z)$ is the CMB temperature at z; and $T_{\rm S}$ is the spin temperature of hydrogen at z. $T_{\rm S}$ is an effective temperature that describes the relative abundances of the ground and excited states of the hyperfine splitting (spin-flip transition) of the hydrogen atom. In the absence of astrophysical radiation, this temperature is defined by collisions of the hydrogen atoms with each other and scattering of CMB photons[11], and therefore $T_{\rm gas}\leq T_{\rm S}\leq T_{\rm CMB}$, where $T_{\rm gas}$ is the (kinetic) temperature of the gas.

Observations of the 21-cm line can be used to probe density fluctuations[12], cosmic reionization[13] and X-ray heating[1,14,15], but the earliest observable feature from cosmic dawn is an absorption signal[1–4] that originates from the indirect coupling of $T_{\rm S}$ to $T_{\rm gas}$ by stellar Lyman-α photons via the Wouthuysen–Field effect[16,17]. The first detection of a cosmic 21-cm signal was made by the Experiment to Detect the Global Epoch of reionization Signature (EDGES)[5], which detected the signal's global spectrum from cosmic dawn and found an absorption peak at frequency $\nu=78\pm1$ MHz ($z=17.2$) with brightness temperature $T_{21}=-500^{+200}_{-500}$ mK; the uncertainties represent 99% confidence intervals and include both thermal and systematic noise. This absorption signal has passed robustness tests for variations in the hardware and processing configuration. If confirmed, this signal (which is 3.8σ below -209 mK, where σ is the standard deviation; the strongest possible absorption at this frequency under standard expectations) cannot be explained without a new dark-matter interaction, even if we take exotic astrophysics into account (see Methods). Indeed, $T_{21}=-300$ mK at $z=17.2$ implies $T_{\rm gas}<5.1$ K, whereas the lowest possible value in the standard scenario is 7.0 K. Basic thermodynamics suggests that it is easy to heat the cosmic gas but difficult to cool it. The extra cooling indicated by the data is possible only through the interaction of the baryons with something even colder.

The only known cosmic constituent that can be colder than the early cosmic gas is dark matter. The reason for this is that dark matter is assumed to interact with itself and with baryons mainly gravitationally, and so it is expected to decouple thermally in the very early Universe and cool down thereafter (very quickly if it is non-relativistic early on, as in the case of cold dark matter). Substantial electrodynamic or nuclear interactions of dark matter would be inconsistent with the observational successes of standard cosmology, including Big Bang nucleosynthesis, CMB observations and the formation and distribution of galaxies. However, weak, non-gravitational interactions are possible. There is a wide array of possibilities for how the strength of such an interaction might vary with temperature or, more specifically, with the velocity v of the scattering baryon relative to the dark-matter particle. Cosmic dawn presents unique physical conditions that can be used to probe a range of parameters that are encountered nowhere else. Specifically, at cosmic dawn, the cosmic gas is at its coldest: it was hotter before owing to its remnant thermal energy from the Big Bang and afterwards owing to X-rays and other heating radiation from astrophysical objects. Therefore, if baryon–dark matter scattering is strongest at low relative velocities, then its effect might be evident only at cosmic dawn.

The cross-section for baryon–dark matter collisions is normally expressed with respect to a relative velocity normalized by the speed of light, and is denoted σ_c. Here, we express it as σ_1, which uses a fiducial relative velocity of 1 km s^{-1}, similar to the typical velocities of baryons and dark-matter particles at cosmic dawn (although in some models they can be less than 0.1 km s^{-1}). We adopt a v^{-4} dependence of the cross-section, which has often been used to illustrate a strongly increasing cross-section with decreasing velocities

$$\sigma(v)=\sigma_c\left(\frac{v}{c}\right)^{-4}=\sigma_1\left(\frac{v}{1\,{\rm km\,s^{-1}}}\right)^{-4} \quad (2)$$

Such a velocity dependence would arise naturally in the case of Rutherford (or Coulomb) scattering. However, the millicharge model,

[1]Raymond and Beverly Sackler School of Physics and Astronomy, Tel Aviv University, Tel Aviv 69978, Israel.

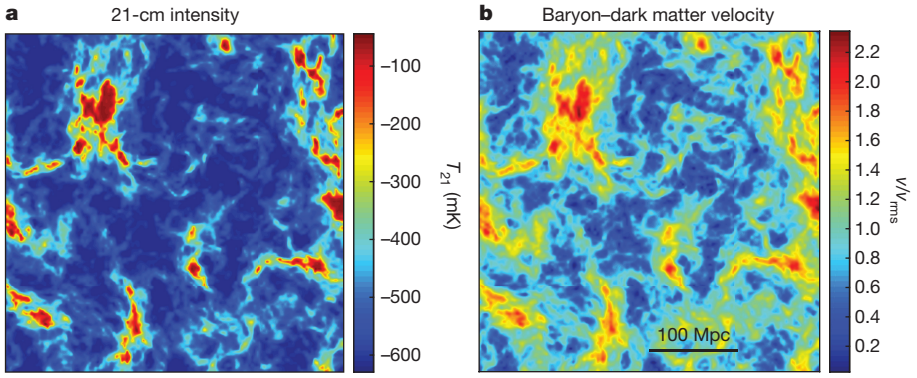

Figure 1 | Simulated 21-cm intensity using a model with baryon–dark matter scattering. a, The 21-cm-transition brightness temperature T_{21} (in millikelvin) in a two-dimensional slice (thickness of 3 Mpc) of a simulated volume of the Universe with sides of 384 Mpc (all lengths co-moving). We consider $z = 17$ ($\nu = 78.9$ MHz), where this model (with $\sigma_1 = 8 \times 10^{-20}$ cm^2 and dark-matter particle mass $m_\chi = 0.3$ GeV) reaches its maximum global 21-cm absorption depth of −504 mK (roughly matching the most likely observed value[5]). This astrophysical model is based on a semi-numerical simulation[15] (see Methods). The spatial 21-cm-signal pattern is determined by the baryon–dark matter relative velocity left over from early cosmic evolution before recombination. **b**, Distribution of the baryon–dark matter relative velocity (in the same simulated volume as that shown in **a**, assuming adiabatic initial density fluctuations), normalized by its r.m.s. value of 29 km s^{-1} at $1 + z = 1{,}010$.

in which dark matter has a small electric charge, is probably ruled out[8,18,19] (see Methods), so we assume a non-standard Coulomb-like interaction between dark-matter particles and baryons that does not depend on whether the baryons are free or bound within atoms.

We calculate the thermal evolution of the baryons and the dark matter by following the exchange of energy and momentum between them[8–10], in which their relative velocity after cosmic recombination has an important role[10]. This velocity remnant[20] arises from the fact that the motion of dark matter is determined by gravity, whereas baryons scatter rapidly off the CMB photons and move along with them in their acoustic oscillations prior to cosmic recombination. This relative velocity (also called the streaming velocity) has received attention recently owing to its effect on early galaxy formation[21], which may produce an observable 21-cm signature[22,23]. However, here we consider baryon–dark matter scattering that depends on the particle velocities directly, not their effect on galaxies.

The baryon–dark matter relative velocity varies spatially (Fig. 1), with a large-scale pattern of coherent regions[21] of about 100 Mpc across. Because the root-mean-square (r.m.s.) velocity is supersonic (decreasing from a Mach number of about 5 right after recombination to approximately 2 when the gas thermally decouples from the CMB) and the scattering cross-section (equation (2)) varies with the relative velocity, the evolution in each region depends strongly on the local value of the initial velocity[10]. At high relative velocities, scattering is weaker (at least until the relative velocity is dissipated by the scattering) and the kinetic energy of the system is partially used to heat the baryons; consequently, a higher relative velocity usually implies less cooling. The dependence of the cooling on velocity results in order-unity fluctuations of the 21-cm intensity(Fig. 1), which we average over (using a Maxwellian distribution for the magnitude of the relative velocity[21]) to estimate the global 21-cm signal.

Such a calculation has been done previously[10], but only for the dark ages, before the formation of any astrophysical sources. In that regime, baryon–dark matter scattering can yield substantial absorption (see the $\nu < 33$ MHz part of the graph in Fig. 2, where previously calculated curves reach a brightness temperature no lower than −70 mK). However, this is unlikely to be observable in the foreseeable future because such low-frequency observations are very difficult to obtain because of ionospheric distortions and because the Galactic synchrotron foreground[3] at $\nu = 20$ MHz is about 40 times stronger than at $\nu = 80$ MHz. A purely cosmological signal would disappear after the dark ages (at $\nu \approx 50$ MHz) because the expansion of the Universe and the cooling of the gas make the coupling of the 21-cm line to $T_{\rm gas}$ (through atomic collisions) less effective than that to the CMB. This drives $T_{\rm S}$ closer to $T_{\rm CMB}$ and eliminates the 21-cm signal.

By combining baryon–dark matter scattering with radiation emitted from the first stars during cosmic dawn in our calculations, we find strong 21-cm absorption that can explain the feature measured by EDGES (Fig. 2). The existence and shape of this absorption dip can be attributed to early astrophysically generated Lyman-α and X-ray radiation backgrounds; this conclusion is consistent with observations that have not detected a strong absorption signal at higher frequencies (see Methods). At the same time, the unexpectedly large depth of the 21-cm absorption indicates cosmic gas that has been cooled substantially by baryon–dark matter scattering. This suggests that only a combination of the two ideas can account for the EDGES data.

The observed 21-cm signal can be explained by considering wide ranges of dark-matter particle masses and baryon–dark matter scattering cross-sections (Fig. 3). Assuming a minimum absorption of −300 mK (as measured[5] at a 99% confidence level), the dark-matter particle must be lighter than 4.3 GeV, which is well below the mass of about 100 GeV that is commonly expected for a weakly interacting massive particle. This finding is consistent with the lack of a direct detection of dark-matter particles by detectors that are sensitive to a wide range of possible weakly interacting massive particles[24,25]. There is no lower limit on the mass except for the extreme limit derived by considering ultra-light ('fuzzy') dark matter[26], namely, $m_\chi \approx 10^{-31}$ GeV, where m_χ is the mass of the dark-matter particle. The same observational result also implies that the scattering cross-section σ_1 is greater than 3.4×10^{-21} cm^2; for the $\sigma(v) \propto v^{-4}$ model (equation (2)), this corresponds to $\sigma_c > 4.2 \times 10^{-43}$ cm^2. Because there is no maximum cross-section, cosmic dawn observations are sensitive to an enormous part of the dark-matter parameter space (in terms of particle mass and cross-section), much of which is unavailable to other probes (see Methods).

The observed signal also places a direct limit on early-Universe scenarios in which dark matter is not completely cold, that is, has a relic thermal velocity. Because dark matter must be colder than baryons in order to cool them, if we demand it to be colder than $T_{[17]}$ (its temperature at $z = 17$), then its r.m.s. velocity at $1 + z = 1{,}010$ must be $v_{\rm rms}^{1010} < (16\,{\rm km\,s^{-1}})\sqrt{T_{[17]}/(5\,{\rm K})}\,\sqrt{(1\,{\rm GeV})/m_\chi}$. In addition, in order for the dark matter to cool the gas at cosmic dawn substantially without disrupting the CMB too much, it must reach a thermal velocity of at most a few kilometres per second at $z = 17$, which puts an upper limit (independent of m_χ) of about 150 km s^{-1} on $v_{\rm rms}^{1010}$. Current limits on warm dark matter[27] allow models with $m_\chi \approx 3$ keV, which have a corresponding $v_{\rm rms}^{1010} \approx 10$ km s^{-1}. Such thermal motion is very far from these upper limits but is comparable to the baryon–dark matter relative velocity, which dominates the 21-cm pattern (Fig. 1); thus, it may be detected or ruled out by observations of 21-cm fluctuations. For

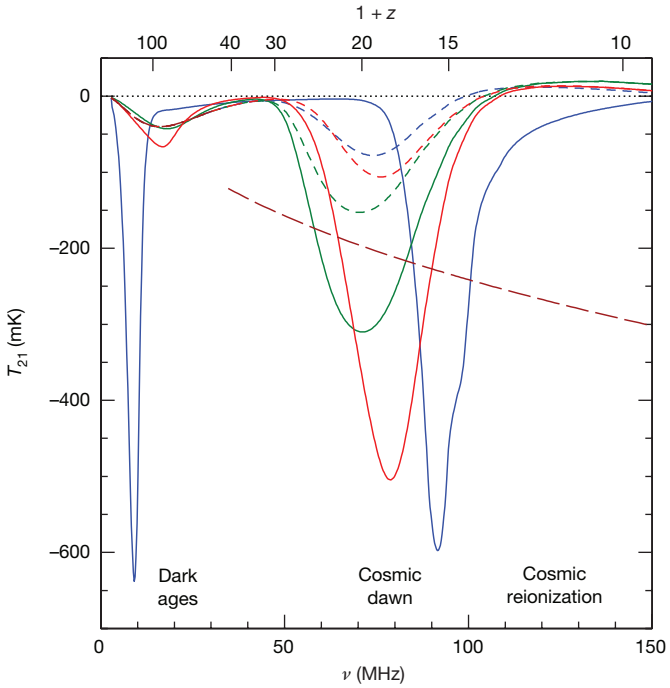

Figure 2 | Global 21-cm signal in models with baryon–dark matter scattering. The globally averaged 21-cm brightness temperature T_{21} (in millikelvin) is shown at an observed frequency ν (in megahertz), with the corresponding value of $1+z$ displayed at the top. We chart some of the space of possible 21-cm signals (see Methods for a discussion on their shapes) using three models (solid curves), with: $\sigma_1 = 8\times10^{-20}$ cm^2 and $m_\chi = 0.3$ GeV (red; roughly matching the most likely observed value[5] of the peak absorption); $\sigma_1 = 3\times10^{-19}$ cm^2 and $m_\chi = 2$ GeV (green); and $\sigma_1 = 1\times10^{-18}$ cm^2 and $m_\chi = 0.01$ GeV (blue). The astrophysical parameters assumed by these models are given in Methods. The corresponding 21-cm signals in the absence of baryon–dark matter scattering are shown as short-dashed curves. Also shown for comparison (brown long-dashed line) is the standard prediction for future dark ages measurements assuming no baryon–dark matter scattering for $\nu < 33$ MHz (matches all the short-dashed curves in this range) and the lowest global 21-cm signal at each redshift that is possible with no baryon–dark matter scattering, regardless of the astrophysical parameters used (for $\nu > 33$ MHz).

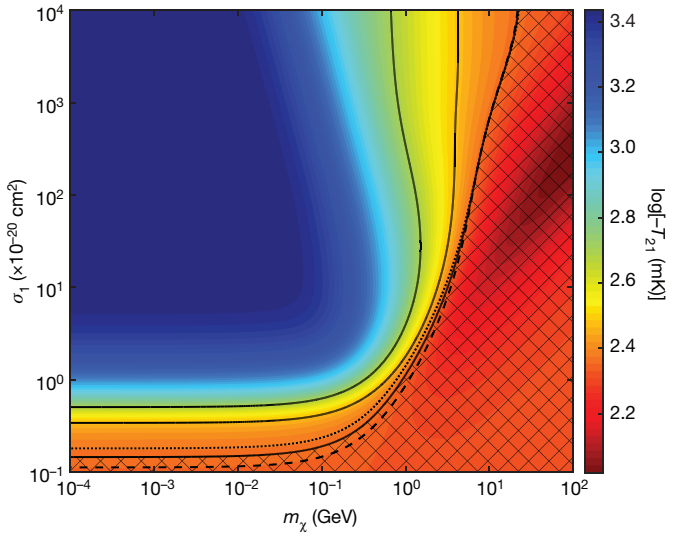

Figure 3 | Constraints on dark-matter properties using cosmic dawn observations. The minimum possible 21-cm brightness temperature T_{21} (expressed as the logarithm of its absolute value) is shown at $z = 17$ ($\nu = 78.9$ MHz), regardless of the astrophysical parameters used (that is, assuming saturated Lyman-α coupling and no X-ray heating), as a function of m_χ and σ_1 (equation (2)). Also shown (solid black curves) are contours corresponding to the following values of T_{21} (from right to left): −231 mK, which corresponds to 10% stronger absorption than the highest value obtained without baryon–dark matter scattering (−210 mK at $z = 17$, or 2.32 on the logarithmic scale); −300 mK, which is the minimal absorption depth in the data at a 99% confidence level; and −500 mK, the most likely absorption depth in the data. The hatched region is excluded if we assume absorption[5] by at least −231 mK at $z = 17$; this 3.5σ observational result implies $\sigma_1 > 1.5\times10^{-21}$ cm^2 (corresponding to $\sigma_c > 1.9\times10^{-43}$ cm^2 for $\sigma(v) \propto v^{-4}$) and $m_\chi < 23$ GeV. (Although any m_χ above a few gigaelectronvolts requires high σ_1, this parameter combination could be in conflict with other constraints; see Methods.) If we adopt the observed minimum absorption of $T_{21} = -300$ mK, then (again, regardless of astrophysics) the dark matter must satisfy $\sigma_1 > 3.4\times10^{-21}$ cm^2 ($\sigma_c > 4.2\times10^{-43}$ cm^2) and $m_\chi < 4.3$ GeV; a brightness temperature of −500 mK implies $\sigma_1 > 5.0\times10^{-21}$ cm^2 ($\sigma_c > 6.2\times10^{-43}$ cm^2) and $m_\chi < 1.5$ GeV. We also illustrate the redshift dependence of these limits via the corresponding 10% contours at $z = 14$ (dashed) and $z = 20$ (dotted).

dark matter that is initially cold, the thermal motion generated by baryon–dark matter scattering may produce effects similar to those predicted by models of warm dark matter (see Methods).

Astronomical testing of the observed signal[5] and of its interpretation in terms of baryon–dark matter scattering will probably begin with other global 21-cm experiments, such as the Shaped Antenna Measurement of the Background Radio Spectrum (SARAS)[28] and the Large-Aperture Experiment to Detect the Dark Ages (LEDA)[29], that will attempt to confirm the measured global signal. Additionally, upcoming 21-cm fluctuation experiments aimed at cosmic dawn will provide a definitive test because the expected spatial pattern of the 21-cm intensity should clearly display a transformed version of the spatial pattern of the baryon–dark matter relative velocity (Fig. 1). Experiments such as the Hydrogen Epoch of Reionization Array (HERA)[6] and the Square Kilometre Array (SKA)[7] should be able to measure the corresponding 21-cm power spectrum because the r.m.s. fluctuation predicted by a model that assumes baryon–dark matter scattering (Fig. 1) is 140 mK (the previously expected maximum value was about 20 mK). Moreover, because of its large spatial scale (of the order of 100 co-moving Mpc, which corresponds to half a degree), the fluctuation pattern should be easy to observe, so no high angular resolution is necessary. As in the case of the galaxy-driven effect of the baryon–dark matter relative velocity[21–23], the power spectrum should show a strong signature of the baryon acoustic oscillations (of order unity in this case) because this velocity arises in part from the participation of baryons in the sound waves of the primordial baryon–photon fluid. A precision measurement at cosmic dawn of the scale of the baryon acoustic oscillations (and thus of the angular diameter distances of the corresponding redshifts) would be a useful cosmological tool to add to current constraints that are based on similar measurements from low-redshift galaxy clustering[30]. If most stars form in galactic haloes with masses lower than about 10^7 solar masses at cosmic dawn, then their spatial distribution should show a similar pattern [21–23] and be strongly anti-correlated with the baryon temperature.

The predicted spatial pattern (Fig. 1) should enable 21-cm imaging of cosmic dawn with the SKA, given the expected sensitivity of the array[7]. The probability distribution function of the 21-cm intensity is expected to be a transformed Maxwellian, which is highly asymmetric, and imaging could verify this unanticipated non-Gaussianity directly. Because the presence of dark matter has historically been inferred from the general theory of relativity on galactic and cosmological scales, confirmation of the existence of dark matter would constitute not only a discovery of physics beyond the standard model, but also verification of this theory.

Online Content Methods, along with any additional Extended Data display items and Source Data, are available in the online version of the paper; references unique to these sections appear only in the online paper.

Received 16 July 2017; accepted 23 January 2018.

1. Madau, P., Meiksin, A. & Rees, M. J. 21 centimeter tomography of the intergalactic medium at high redshift. *Astrophys. J.* **475,** 429–444 (1997).
2. Tozzi, P., Madau, P., Meiksin, A. & Rees, M. J. Radio signatures of H i at high redshift: mapping the end of the "dark ages". *Astrophys. J.* **528,** 597–606 (2000).
3. Furlanetto, S. R., Oh, S. P. & Briggs, F. H. Cosmology at low frequencies: the 21 cm transition and the high-redshift Universe. *Phys. Rep.* **433,** 181–301 (2006).
4. Barkana, R. The rise of the first stars: supersonic streaming, radiative feedback, and 21-cm cosmology. *Phys. Rep.* **645,** 1–59 (2016).
5. Bowman, J. D., Rogers, A. E. E., Monsalve, R. A., Mozdzen, T. J. & Mahesh, N. An absorption profile centred at 78 megahertz in the sky-averaged spectrum. *Nature* **555,** https://doi.org/10.1038/nature25792 (2018).
6. DeBoer, D. R. *et al.* Hydrogen Epoch of Reionization Array (HERA). *Publ. Astron. Soc. Pacif.* **129,** 045001 (2017).
7. Koopmans, L. *et al.* The cosmic dawn and epoch of reionisation with SKA. In *Proc. Advancing Astrophysics with the Square Kilometre Array* (Proceedings of Science, 2015).
8. Dvorkin, C., Blum, K. & Kamionkowski, M. Constraining dark matter–baryon scattering with linear cosmology. *Phys. Rev. D* **89,** 023519 (2014).
9. Tashiro, H., Kadota, K. & Silk, J. Effects of dark matter-baryon scattering on redshifted 21 cm signals. *Phys. Rev. D* **90,** 083522 (2014).
10. Muñoz, J. B., Kovetz, E. D. & Ali-Haïmoud, Y. Heating of baryons due to scattering with dark matter during the dark ages. *Phys. Rev. D* **92,** 083528 (2015).
11. Purcell, E. M. & Field, G. B. Influence of collisions upon population of hyperfine states in hydrogen. *Astrophys. J.* **124,** 542–549 (1956).
12. Hogan, C. J. & Rees, M. J. Spectral appearance of non-uniform gas at high *z*. *Mon. Not. R. Astron. Soc.* **188,** 791–798 (1979).
13. Scott, D. & Rees, M. J. The 21-cm line at high redshift: a diagnostic for the origin of large scale structure. *Mon. Not. R. Astron. Soc.* **247,** 510–516 (1990).
14. Furlanetto, S. R. The global 21-centimeter background from high redshifts. *Mon. Not. R. Astron. Soc.* **371,** 867–878 (2006).
15. Fialkov, A., Barkana, R. & Visbal, E. The observable signature of late heating of the Universe during cosmic reionization. *Nature* **506,** 197–199 (2014).
16. Wouthuysen, S. A. On the excitation mechanism of the 21-cm (radio-frequency) interstellar hydrogen emission line. *Astron. J.* **57,** 31–32 (1952).
17. Field, G. B. Excitation of the hydrogen 21-cm line. *Proc. IRE* **46,** 240–250 (1958).
18. Chuzhoy, L., & Kolb, E. W. Reopening the window on charged dark matter. *J. Cosmol. Astropart. Phys.* **7,** 14 (2009).
19. McDermott, S. D., Yu, H.-B. & Zurek, K. M. Turning off the lights: how dark is dark matter? *Phys. Rev. D* **83,** 063509 (2011).
20. Sunyaev, R. A. & Zeldovich, Y. B. Small-scale fluctuations of relic radiation. *Astrophys. Space Sci.* **7,** 3–19 (1970).
21. Tseliakhovich, D. & Hirata, C. Relative velocity of dark matter and baryonic fluids and the formation of the first structures. *Phys. Rev. D* **82,** 083520 (2010).
22. Dalal, N., Pen, U.-L. & Seljak, U. Large-scale BAO signatures of the smallest galaxies. *J. Cosmol. Astropart. Phys.* **11,** 7 (2010).
23. Visbal, E., Barkana, R., Fialkov, A., Tseliakhovich, D. & Hirata, C. M. The signature of the first stars in atomic hydrogen at redshift 20. *Nature* **487,** 70–73 (2012).
24. XENON Collaboration. First dark matter search results from the XENON1T experiment. *Phys. Rev. Lett.* **119,** 181301 (2017).
25. PandaX-II Collaboration. Dark matter results from 54-ton-day exposure of PandaX-II experiment. *Phys. Rev. Lett.* **119,** 181302 (2017).
26. Hu, W., Barkana, R. & Gruzinov, A. Fuzzy cold dark matter: the wave properties of ultralight particles. *Phys. Rev. Lett.* **85,** 1158–1161 (2000).
27. Iršič, V. *et al.* New constraints on the free-streaming of warm dark matter from intermediate and small scale Lyman-α forest data. *Phys. Rev. D* **96,** 023522 (2017).
28. Singh, S. *et al.* First results on the epoch of reionization from first light with SARAS 2. *Astrophys. J.* **845,** L12 (2017).
29. Bernardi, G., McQuinn, M. & Greenhill, L. J. Foreground model and antenna calibration errors in the measurement of the sky-averaged λ21 cm signal at $z \sim 20$. *Astrophys. J.* **799,** 90 (2015).
30. Alam, S. *et al.* The clustering of galaxies in the completed SDSS-III Baryon Oscillation Spectroscopic Survey: cosmological analysis of the DR12 galaxy sample. *Mon. Not. R. Astron. Soc.* **470,** 2617–2652 (2017).

Acknowledgements I am grateful to J. Bowman for alerting me to possible indications of very deep absorption in the EDGES results, which inspired this work. This project was made possible through the support of a grant from the John Templeton Foundation. The opinions expressed in this publication are those of the author and do not necessarily reflect the views of the John Templeton Foundation.

METHODS

The measured signal and its theoretical interpretation. In this work we relied on the EDGES measurement of the global 21-cm spectrum from cosmic dawn[5]. The absorption signal was detected with a signal-to-noise ratio of 37. Moreover, the signal was observed in data spanning nearly two years and has passed many robustness tests with little change[5]. Various hardware configurations were tried, including two separately built copies of the instrument, various sizes of the metal ground plane (from 10 m to 30 m on a side), variations in the instrument's orientation and inclusion (or not) of a balun shield. Also, the processing configurations included: two independent processing pipelines (tested with simulated data); various calibration techniques and measurements; inclusion (or not) of beam and balun or ground-plane loss corrections; a four-, five- or six-term foreground polynomial or a different physically motivated five-term foreground model; various frequency intervals (51–99 MHz, 61–99 MHz or 65–95 MHz); and data collected at various sky positions of the Sun, Moon and Galaxy. The measured absorption profile is inconsistent with typical spectra of radio-frequency interference, does not appear Galactic (it is inconsistent with the absorption spectra of H II regions or radio-frequency recombination lines and is not concentrated in the Galactic plane), and is not explained by the ionosphere (which produces a broadband absorption with diurnal variations, as shown by models and observations) or by molecular lines in the atmosphere (which are much too weak).

For the theoretical predictions, we combined a calculation of the effect of baryon–dark matter scattering with a simulation of the effect of the first stars on intergalactic hydrogen. We calculated the thermal exchange between baryons and dark matter by following the evolution of the baryon–dark matter relative velocity (equation (20) in ref. 10) and including heating and cooling terms related to scattering (equations (18) and (19) of ref. 10, using also equations (13), (14) and (16) of the same paper). We treated the baryons as equal-mass particles with 1.22 times the proton mass (which is the mean molecular mass of neutral primordial gas), whereas in ref. 10 one proton mass is used. Thus, equation (2) effectively represents the cross-section of the scattering between dark matter and an average baryon. In reality, the treatment of helium is probably complicated and highly model-dependent[8]. We started our calculation at kinematic decoupling ($1+z=1{,}010$), as in previous calculations[10], and we confirmed that starting earlier would not affect our results much at lower redshifts.

In addition to baryon–dark matter scattering, at each redshift we included spatially uniform backgrounds of astrophysical radiation of the three types that are important in 21-cm cosmology (Lyman-α photons, X-rays and ionizing photons). More precisely, we used the volume-averaged values of Lyman-α coupling (before low-temperature corrections), the rate of heating due to X-rays and the ionized fraction, all taken from a semi-numerical simulation[15,31] with astrophysical parameters chosen to illustrate absorption dips that are consistent with the observed signal. In the model used to obtain the results shown in Fig. 1 and the red curve in Fig. 2, star formation occurs only in haloes that allow atomic cooling and with an efficiency of $f_*=1.58\%$, and X-rays normalized on the basis of low-redshift observations are emitted with a soft power-law spectrum. The green curve in Fig. 2 is obtained with the same model, except that the efficiency of the production of Lyman-α photons is 10 times higher. The model that gives the blue curve in Fig. 2 assumes the same parameters as the model that obtains the red curve but considers an efficiency of $f_*=0.5\%$ and assumes that star formation occurs in haloes that allow molecular cooling. Moreover, it considers an X-ray efficiency 4 times higher than that of the model of the red curve and an X-ray spectrum that extends down to 0.1 keV instead of 0.2 keV. Astrophysical radiation fields are expected to vary spatially, leading to 21-cm fluctuations during cosmic dawn due to Lyman-α fluctuations[32] and X-ray heating fluctuations[33]; these are sizeable and potentially observable. However, we neglected these fluctuations here because of the much larger ones that result from baryon–dark matter scattering. Throughout the analysis, we assumed the known values of the cosmological parameters[34], $\Omega_m=0.307$, $\Omega_b=0.0482$ and $h=0.678$.

In most of the model space, the theoretically predicted dip in the cosmic-dawn absorption curve shown in Fig. 2 is well fitted by a simple Gaussian (although for the blue solid curve in Fig. 2, this is true only for the deepest portion of the absorption feature). The measurement of ref. 5 favours a different flattened-Gaussian shape but systematic variations in the hardware configuration weaken this conclusion. In figure 2 of ref. 5, two of the six plotted best-fit profiles and residuals are not very flattened. The data fits show an anticorrelation between the degree of flattening and the absorption amplitude; low flattening (as suggested by the theoretical models) favours high amplitudes of around 1,000 mK.

Strongest possible absorption without baryon–dark matter scattering. A measurement of stronger-than-expected absorption is evidence of the existence of dark matter, as such absorption cannot be produced without baryon–dark matter scattering. In the standard picture, the best-case scenario for producing strong 21-cm absorption is to assume no reionization ($x_{HI}=1$ in equation (1)), saturated coupling ($T_S=T_{gas}$) and no astrophysical heating. In this case, the gas at high redshifts is colder than the CMB because its adiabatic cooling is faster. However, the baryons are thermally coupled to the CMB through Compton heating until $z\approx150$. This well understood phenomenon yields[35] a strongest possible absorption signal (regardless of the uncertain astrophysics at high redshift) of $T_{21}=-209$ mK at $\nu=78$ MHz. We note that this maximum possible absorption is an extreme value (in the standard case without baryon–dark matter scattering) that would not be considered very likely. Models with various astrophysical parameter values[31] predict T_{21} values at $\nu=78$ MHz that range from -209 mK up to positive values, with most of them between -150 mK and -50 mK. More generally, the most negative global 21-cm signal at each frequency that would be possible with no baryon–dark matter scattering (regardless of the parameters of high-redshift astrophysics) is shown (at $\nu>33$ MHz) by the brown long-dashed curve in Fig. 2.

We consider various ideas for increasing the absorption without baryon–dark matter interactions. Fluctuations in the gas density ρ_g affect the 21-cm signal, as the absorption strength is proportional to ρ_g. However, adiabatic heating with $T_{gas}\propto\rho_g^{2/3}$ counteracts this and leads to only a small increase in the absorption in overdense regions, whereas in the voids these factors combine to weaken the overall absorption. Actually, linear fluctuations are symmetric and cancel out when averaged globally over overdense and underdense regions. To change the observed global signal, nonlinear fluctuations are needed. The regime of mildly nonlinear density fluctuations is well understood, as it corresponds to the sheets and filaments of the cosmic web that successfully explain[36] the observed properties of the Lyman-α forest at $z=2$–5. At cosmic dawn, the Universe was probably much more homogeneous than at $z=2$–5 and had less-nonlinear density fluctuations because gravity had not had as much time to drive the growth of fluctuations. Nevertheless, even if we were to assume that somehow the density fluctuations corresponding to the Lyman-α forest were already in place at $z\approx20$, this still would not produce a larger absorption signal than in the absence of such density fluctuations. To check this quantitatively, we assume the best case of $T_S=T_{gas}$ and adiabatic heating and cooling, and we average the 21-cm brightness temperature over the density distribution at $z=2$–6 in simulations that match Lyman-α observations[37]. The result is a weaker average absorption than would occur in the absence of density fluctuations. More evidence that density fluctuations do not produce unusual absorption comes from numerical simulations of the Universe at cosmic dawn; these have been run on various volumes and at various resolutions[38–40], and none of them has predicted a stronger globally averaged absorption signal than the simple limit shown by the brown long-dashed curve in Fig. 2.

Under standard cosmology, the total gas fraction within virialized haloes at $z=20$ is expected to be below 1% because the intergalactic gas can only collect in haloes of mass at least equal to the filtering mass[41,42] of about 3×10^4 solar masses. We can consider, though, an exotic scenario where unexpectedly large density fluctuations on small scales would produce a much larger abundance of early haloes. This would not produce more absorption either. The lowest T_{gas} at $z=20$ in the standard scenario is about 9 K at the cosmic mean density. As the gas is heated adiabatically, it reaches the CMB temperature (57 K at $z=20$) at an overdensity of 16. After that point it contributes extra emission, not absorption. When the gas enters a virialized halo, it is probably shock-heated. If it cools efficiently, primordial cooling via molecular hydrogen is effective only down to temperatures of a few hundred kelvin and, in any case, efficient cooling probably leads to star formation and even more heating. We also note that the 21-cm optical depth of the coldest-possible gas (without baryon–dark matter scattering) is $\tau_{21}\approx10\%$ at the mean density at $z=20$; this varies as $\tau_{21}\propto\rho_g/T_{gas}\propto\rho_g^{1/3}$, assuming adiabatic evolution. This means that only very dense gas (inside virialized haloes) can be optically thick, and such gas is expected to be hot.

Another possibility is to change the residual electron fraction after recombination, which determines the rate of Compton heating that keeps the gas close to the CMB temperature until $z\approx150$. To produce unusually strong absorption, such as $T_{21}=-300$ mK at $\nu=77$ MHz, the gas would need to decouple thermally at a value of $1+z$ that is larger by a factor of 1.4 than that predicted by standard cosmology; this would happen if the residual ionized fraction were lower than expected by a factor of about 4. Before cosmic recombination, the gas is strongly coupled to the CMB and cannot cluster, so it would probably be unaffected even by exotic physics, such as unusually strong dark-matter clumping. After the freeze-out at the end of cosmic recombination, the recombination time continues to increase as $1/\rho_g$, so the residual electron fraction changes slowly with time and is only weakly dependent on density (in part because the recombination coefficient declines with temperature and the temperature rises with density). It is difficult to imagine something that could lower the mean residual electron fraction by a large factor.

More generally, it would be difficult to change the basic cosmological parameters, the cosmic expansion history or the physics involved in cosmic recombination

substantially. These inputs are strongly constrained by the success of standard cosmology in fitting observations of the CMB plus low-redshift observations. Proposed exotic astrophysics or physics concepts—such as unexpected populations of stars or black holes, or dark-matter annihilation or decay—also cannot explain the stronger absorption. Such scenarios would generate extra ultraviolet, X-ray or γ-ray radiation, which would generate more heating as well as more ionization (which would lower $x_{\rm HI}$ and also boost the Compton heating of the gas). Also, Lyman-α coupling cannot be stronger than the saturated coupling limit ($T_{\rm S}=T_{\rm gas}$) that we have considered here.

Astrophysical considerations and implications. While the detailed parameters of the astrophysical sources at high redshift are highly uncertain, strong 21-cm absorption is a generic prediction. A scan through a wide range of currently plausible astrophysical parameter values[31] (without baryon–dark matter scattering) shows that all models feature an absorption dip at cosmic dawn[14], which is produced (in the direction of increasing ν) by a fall (that is, increasing absorption) due to increasing Lyman-α coupling, followed by a rise caused by increasing X-ray heating (or due to reionization in models with late X-ray heating). The depth of the absorption dip[31] is in the range $-240\,{\rm mK}<T_{21,\rm min}<-25\,{\rm mK}$, and its position is in the range $52\,{\rm MHz}<\nu_{\rm min}<120\,{\rm MHz}$ (corresponding to $11<z_{\rm min}<26.5$).

Once baryon–dark matter scattering is included, the observed global 21-cm signal is determined by the complex interplay of this scattering with astrophysics. For example, in the large region (Fig. 3) of low m_χ and high σ_1 that is allowed, the initial cooling due to baryon–dark matter scattering can be extremely effective and lead to global 21-cm absorption as strong as $-600\,{\rm mK}$ in the dark ages (but only at very high redshifts, higher than 100). In these models, the gas is so cold that Lyman-α coupling is delayed owing to low-temperature corrections (discussed below), and cosmic heating is also delayed because X-ray heating must initially counteract the baryon–dark matter cooling. In this region of parameter space, astrophysical models can be chosen to produce an absorption peak position and depth that agree with the data[5], but detailed parameter constraints require full consideration of the large variety of possible astrophysical parameters, which we leave for future work. We also note that a very high σ_1 would tend to suppress the baryon–dark matter relative velocity and, with it, the associated fluctuations (discussed in the main text); although the normal 21-cm fluctuations due to inhomogeneous galaxy formation would be enhanced in proportion to the (unexpectedly large) absolute value of the mean global signal.

The observed global 21-cm signal[5] represents the first detection of some of the earliest stars. The location of the peak absorption at $z\approx17$ is not surprising, but it considerably narrows down astrophysical parameters that were previously almost unconstrained. In general, the maximal absorption corresponds to the late stages of Lyman-α coupling, together with the early stages of X-ray heating. The observed timing of these astrophysical cosmic milestones is well within the expected range of astrophysical parameters[31], which further supports the dark-matter-cooling interpretation, as there is no indication of exotic astrophysics. Interestingly, this early heating is also consistent with limits (obtained from 21-cm observations during the epoch of reionization) on both the global and fluctuation signals[28,43,44], which disfavour strong absorption at low redshifts (such absorption is expected in the case of late heating). Indeed, the detected signal implies that future 21-cm observations should focus on cosmic dawn, where the 21-cm signal (both the global signal and the power spectrum) is probably much stronger than previously expected, and not on the later era of cosmic reionization, which has been the focus thus far[28,43–47] and where the signal strength is probably in the lower part of the previously expected range.

The Lyman-α coupling of the 21-cm line is known to become less effective when the gas temperature is low[4,48–51]. In the previously standard case, these low-temperature corrections amount at most to a 20% reduction in the coupling at any redshift[4]. With the lower gas temperatures encountered in the case of substantial baryon–dark matter scattering, however, the low-temperature corrections can reduce the coupling by an order of magnitude or more, delaying strong Lyman-α coupling and greatly changing the global 21-cm signal. Indeed, in some models the gas temperature is so low ($<0.1\,{\rm K}$) that these low-temperature corrections (as well as additional basic physics of 21-cm cosmology) may need to be re-assessed. Furthermore, the standard expression for the 21-cm signal (equation (1)) is a linearization that assumes a low 21-cm optical depth (a valid assumption if there is no baryon–dark matter scattering), but here we encounter high optical depth values and thus use the more general expression[1]. Lyman-α scattering can also affect the thermal state of the cosmic gas; for almost all reasonable astrophysical parameters[49,52], heating due to continuum photons dominates over cooling from injected photons (for gas below about 100 K) and the heating rate is weak compared to that of X-ray heating.

Substantial baryon–dark matter scattering would also influence the formation of the first stars. The lower gas temperature would reduce the Jeans mass, and the dissipation of the baryon–dark matter relative velocity would reduce its suppression effects on star formation. Both of these effects would boost star formation relative to the case of no baryon–dark matter scattering, but their impact might be limited because of the large time scales needed for galaxy formation. Baryon infall into dark-matter haloes begins at recombination, and for most dark-matter parameter values it takes some time until the baryon–dark matter scattering has a considerable effect. We have neglected effects on galaxy formation in this work because they are dwarfed by the direct effect of excess gas cooling on the 21-cm signal.

The range of dark-matter properties that can be probed by cosmic dawn observations. The dark-matter parameters that affect 21-cm cosmology are shown in Fig. 3, but it is important to understand the basic physics behind these constraints. In particular, we can understand why there is an upper limit on the mass of a dark-matter particle that can cool cosmic baryons by considering the maximum possible cooling. As mentioned previously, baryons thermally decoupled from the CMB at $z\approx150$. In the presence of baryon–dark matter scattering, by that time the dark matter had acquired a non-zero temperature T_χ; however, $T_\chi\ll T_{\rm gas}$ is required for maximum cooling of the baryons at this time. For cooling to occur, the two fluids must be strongly coupled after the baryons thermally decouple, so that the baryons share some of their energy with the dark matter. The most that such coupling can achieve, if it is strong, is a thermal equilibrium, at which both the baryons and the dark matter have a common (time-dependent) temperature $T_{\rm fin}$. Then at a given time, the relation between the baryon temperature $T_{\rm gas}$ in the absence of baryon–dark matter scattering and the lowest possible temperature $T_{\rm fin}$ with scattering is given by conservation of energy (per unit volume) as

$$T_{\rm fin}=T_{\rm gas}\frac{n_{\rm b}}{n_{\rm b}+n_\chi}=\frac{T_{\rm gas}}{1+(\rho_\chi/\rho_{\rm b})(\mu_{\rm b}/m_\chi)}\approx\frac{T_{\rm gas}}{1+(6\ {\rm GeV})/m_\chi} \qquad (3)$$

where $n_{\rm b}$ and n_χ are the number densities of baryons and dark matter, respectively, $\rho_{\rm b}$ and ρ_χ are the corresponding (mean) densities, $\mu_{\rm b}$ is the mean baryonic mass and m_χ is the mass of a dark-matter particle. Although we have neglected the effect of the initial baryon–dark matter relative velocity, the kinetic energy associated with it would only produce more heating. As an example, to reach $T_{21}=-300\,{\rm mK}$ at $z=17$ (the current limit at 99% confidence[5]), the simple estimate in equation (3) yields a maximum possible m_χ of 16 GeV. In reality, the cooling never reaches the best-case scenario assumed in this simple estimate, and we find an actual maximum mass of 4.3 GeV (see Fig. 3).

There is no lower limit on the mass of the dark-matter particle that can affect the 21-cm signal, because the cooling rate becomes independent of m_χ when $m_\chi\ll\mu_{\rm b}$. In that limit, the energy lost by a baryon per collision (at a given baryon–dark matter relative velocity) is proportional to m_χ and the scattering rate is proportional to $n_\chi\sigma_1$; therefore, the total cooling rate is proportional to $\rho_\chi\sigma_1$, where ρ_χ is the known mean density of dark matter. Thus, a substantial interaction requires a minimum σ_1 that is independent of m_χ when $m_\chi\ll\mu_{\rm b}$ (Fig. 3). We note that the enormous range of particle masses (as well as scattering cross-sections) that are potentially detectable by cosmic dawn observations can be considered an argument that such a detection is not an unreasonable possibility.

The dependence of the effectiveness of the baryonic cooling on the baryon–dark matter scattering cross-section is non-trivial. A higher cross-section means that more of the thermal energy of the baryons can be transferred to the dark matter; on the other hand, it also implies that the dark matter warms up earlier on, before thermal decoupling of the gas from the CMB, which reduces the ability of the dark matter to later cool the gas. There is even a region (for example, $\sigma_1=2\times10^{-18}\,{\rm cm}^2$ and $m_\chi=100\,{\rm GeV}$; see Fig. 3) where the baryon–dark matter interaction causes a small net baryonic heating due to another effect, namely, the transfer of kinetic energy from their relative velocity to the random gas motions. In the limit of very low m_χ and very high σ_1 (the top-left portion of Fig. 3), the absorption (which is defined with respect to the CMB at zero redshift) approaches its maximum possible value, namely, the CMB temperature of 2.725 K.

Another issue is the effect of baryon–dark matter scattering on the dark matter. According to equation (3), the maximum velocity dispersion, v_χ, of the dark matter (even if it is initially completely cold) relative to the velocity dispersion of the gas, $v_{\rm b}$, in the absence of baryon–dark matter scattering is:

$$\frac{v_\chi}{v_{\rm b}}=\sqrt{\frac{T_{\rm fin}/m_\chi}{T_{\rm gas}/\mu_{\rm b}}}=\left(5+\frac{m_\chi}{1.1\ {\rm GeV}}\right)^{-1/2} \qquad (4)$$

In reality, the dark matter can have a velocity dispersion that is very different at a given time from that corresponding to $T_{\rm fin}$ of equation (3). A higher v_χ can be caused by memory of earlier times—in particular, of the higher temperature of the gas when it was thermally coupled to the CMB—because after decoupling the dark

matter may not be able to cool fast enough to forget its history effectively (the fastest it can cool is adiabatically). Later, once X-rays (and eventually reionization) heat the gas, v_χ can remain low even when v_b rises, as the increasing v_b weakens the baryon–dark matter scattering (assuming the $\sigma(v) \propto v^{-4}$ model). Numerically, we find that v_χ decreases with time but the matter power spectrum may be suppressed by the thermal velocity that exists at high redshifts, when linear growth critical for the later emergence of structure occurs. This may offer a way to alleviate the small-scale crisis of cold dark matter (that is, the model's difficulties in matching the observed properties of dwarf galaxies) that has led to models such as those of warm dark matter and fuzzy dark matter[26,27,53], and can help to set upper limits on the baryon–dark matter cross-section[8]. Allowed models of warm dark matter have $v_{rms} \approx 5\,km\,s^{-1}$ at $z = 500$, so we estimate that models with a similar v_χ at that redshift may also have a considerable effect on the Lyman-α forest or on dwarf galaxies at low redshift. In regions with zero initial streaming velocity, this value of v_χ occurs for $\sigma_1 \approx 10^{-18}\,cm^2$ as long as $m_\chi \ll 1$ GeV (the σ_1 required rises by a factor of 10 for $m_\chi = 1$ GeV); if σ_1 is ten times lower, then v_χ drops to $2\,km\,s^{-1}$ at $z = 500$.

We have assumed throughout this work that $\sigma(v) \propto v^{-4}$ but the velocity dependence of the cross-section can be explored with future 21-cm data. Further global 21-cm measurements may help but will probably not resolve the degeneracies between the dark-matter parameters (cross-section amplitude, velocity dependence and particle mass) and the astrophysical parameters (the X-ray spectrum and the normalization and redshift evolution of the various radiation backgrounds, as determined by parameters related to galaxy formation). Detailed measurements of 21-cm fluctuations, including the 21-cm power spectrum, would provide much more information. For example, the level of the fluctuations caused by the spatially varying baryon–dark matter relative velocity (Fig. 1) depends directly on how rapidly the scattering cross-section varies with velocity. In this regard, it is important to note that while in this study we have focused on the global 21-cm signal, the corresponding 21-cm fluctuations are also (over most of the parameter space shown in Fig. 3) much larger than would be expected in the absence of baryon–dark matter scattering. A more advanced test of $\sigma(v) \propto v^{-4}$ would be a comparison with a measurement of the signal during the dark ages (Fig. 2), which would involve different velocities and would provide constraints independent of astrophysics. However, even the proposed Dark Ages Radio Explorer (DARE) satellite[54] is planned to perform measurements only at frequencies greater than 40 MHz, whereas the predicted absorption signal from the dark ages is expected at 10–30 MHz.

Dark-matter millicharge and other dark-matter models. We have assumed a relatively simple model for the dark matter and its interactions with ordinary matter. However, this model is only an illustration; the EDGES data suggest a low-velocity baryon–dark matter interaction, but do not yet determine the specific form of this interaction. If the measured signal is confirmed and 21-cm cosmology becomes a dark-matter detector, then a wide range of candidate dark-matter models will need to be re-assessed. Examples include models that describe the interaction of dark matter with electrons[55,56] and interactions (with either baryons or electrons) that depend on whether standard-model particles are free or bound within atoms, models in which the dark matter consists of multiple components so that only a fraction of the particles interact with baryons, and models in which dark matter also self-interacts[57]. We add here a few notes on these possibilities. Dark-matter interactions with electrons are currently constrained[56] to lower masses than for interactions with baryons. Also, the formation of atoms obviously affects the motion of electrons much more than that of the baryons. Thus, although an interaction with baryons may not change much at recombination (as long as the interaction is not electromagnetic), one with electrons would be more likely to change, in a complex and model-dependent way. Now, any interaction that is strong only with free protons or electrons decreases in proportion to the residual electron or proton fraction after cosmic recombination. This means that the effect of dark-matter scattering on baryon cooling during cosmic dawn is suppressed relative to the effect on the CMB by a factor of about 5,000. At a temperature of 5 K (indicated by the EDGES data at $z = 17.2$, as noted in the main text), the r.m.s. velocity of baryons is about $0.3\,km\,s^{-1}$, which is lower than the velocity at cosmic recombination by a factor of about 25. For a v^{-4} model, this makes the cross-section larger by a factor of approximately 500,000. Still, the cooling takes time and is unlikely to be effective unless it begins at velocities well above $1\,km\,s^{-1}$. Thus, this type of model might be ruled out by CMB observations, which are very constraining, even for the model that we assumed in this work (see the next section).

It is interesting to consider the specific dark-matter millicharge model[8,18,19,58,59] that naturally yields a v^{-4} cross-section. In this case, the dark matter has a (small) standard electric charge. Considering only the interaction with protons and the aforementioned suppression factor of 5,000, the minimum dark-matter charge (relative to that of the electron) that would be required to produce the cooling indicated by the EDGES data is $\varepsilon \approx 10^{-6}$. The interaction with electrons can also be considerable if the dark-matter mass is well below 1 GeV, which might allow substantial cooling with values of ε as low as about 10^{-8}. However, the entire range of relevant values may already be ruled out: owing to its interaction with Galactic magnetic fields, millicharge dark matter should have been evacuated from the Milky Way disk (and also blocked from re-entering) if[18,19]

$$10^{-11}\frac{m_\chi}{1\ \mathrm{GeV}} < \varepsilon < 3\times 10^{-4}\left(\frac{m_\chi}{1\ \mathrm{GeV}}\right)^{1/2}$$

However, multiple measurements indicate a non-zero local dark-matter density near the Sun[60], roughly consistent with the expected density from the Milky Way's dark-matter halo. This contradicts the idea that the dark matter was evacuated from the disk and thus rules out the existence of millicharge dark matter over a wide range of parameters (we note that this argument has not been made previously). Furthermore, CMB constraints[8,19,59] yield a conservative upper limit of $\varepsilon \approx 4\times 10^{-6}[m_\chi/(1\,\mathrm{GeV})]^{1/2}$. These observational constraints combine to exclude $\varepsilon > 10^{-11}[m_\chi/(1\,\mathrm{GeV})]$ at all relevant values of m_χ, and this excludes the possibility of substantial cooling at cosmic dawn. The dark-matter millicharge model may be similarly (but independently) ruled out on the basis of the effect that the interaction of dark matter with magnetic fields would have on the dark-matter distribution in galaxy clusters[61]. These constraints all rely on the presence of the electric millicharge directly, while if other properties are assumed (for example, related to the dark-matter annihilation properties), other stringent constraints would also apply[58,59].

Comparing cosmic dawn constraints to other limits on baryon–dark matter interactions. The comparison between cosmic dawn observations for dark-matter detection and constraints from direct detection, accelerators and various astrophysical phenomena is model-dependent. Here we adopt the $\sigma(v) \propto v^{-4}$ model, in which case the parameter spaces of the various approaches overlap, and other searches may be able to detect or rule out a dark-matter particle that is consistent with the 21-cm observations at cosmic dawn. However, a more complex interaction—for example, based on a bound state or resonance that is important only at low velocities—could invalidate any such comparison and make cosmic dawn observations a unique probe. Additional model dependence enters some of the comparisons that involve assumptions about dark-matter annihilation or the spin dependence of the baryon–dark matter scattering.

Limits on the v^{-4} model have been derived previously[19], with the strongest limits based on CMB observations (plus a slight improvement from including clustering based on Lyman-α forest data)[8]. However, the 95% confidence limit equivalent to $\sigma_1 < 2\times 10^{-19}[m_\chi/(1\,\mathrm{GeV})]\ cm^2$ was derived only for $m_\chi \gg m_H$. This calculation must be re-done for lower m_χ and fixed more generally to properly include the spatial variation of the baryon–dark matter relative velocity, which would introduce a CMB pattern that may be partially correlated with the standard one. Here we estimate a very rough correction for low dark-matter masses. In the limit of strong coupling (so that the gas and dark matter have the common temperature of equation (3)), including the contribution (neglected in the above limit) of the dark matter to the relative thermal velocity and assuming that the limit is proportional to v^{-4} gives a modified limit of $\sigma_1 < 2\times 10^{-19}(m_\chi/\mathrm{GeV}) \times [1+(\mu_b/m_\chi)]^2\ cm^2$. Nevertheless, if the coupling is not strong, then $T_\chi < T_{gas}$ and the correction factor may be smaller. We conclude that CMB limits may complement the 21-cm signal by imposing useful upper limits on σ_1, but these limits must be carefully re-calculated. There is also a limit on the baryon–dark matter scattering from spectral distortions of the CMB[55], but these distortions occur at rather high redshifts (and thus high velocities) so are probably not important (and have not been considered) for a cross-section that peaks at low velocities, such as that of the $\sigma(v) \propto v^{-4}$ model.

Another possibility (related to the earlier discussion about the dark-matter velocity dispersion) is that between matter–radiation equality and recombination—a period when fluctuations normally grow in the dark matter but not the baryons—the baryon–dark matter coupling might suppress the growth of fluctuations in the dark matter; this effect could be consistent with CMB observations but also important for the power spectrum at low redshift.

A different limit on baryon–dark matter interactions comes from experiments that attempt to detect dark-matter scattering directly with target nuclei in the laboratory. Assuming typical Milky Way halo speeds, with velocities of about $200\,km\,s^{-1}$, the minimum cross-section $\sigma_1 = 3.4\times 10^{-21}\ cm^2$ required for the cosmological 21-cm effect (Fig. 3) translates (in a v^{-4} model) to $\sigma(200\,km\,s^{-1}) > 2\times 10^{-30}\ cm^2$. This is in the range of cross-sections that are hard to probe with underground detection experiments because at such cross-sections dark-matter particles are expected to lose most of their energy in the Earth's crust before reaching the detector[62]. The Cryogenic Rare Event Search with Superconducting Thermometers (CRESST) underground experiment is

most relevant to the 21-cm parameter region, although it constrains only relatively high masses. At $m_\chi = 1$–$5\,\mathrm{GeV}$, it rules out (assuming spin-independent interactions throughout this discussion) values of $\sigma(200\,\mathrm{km\,s^{-1}})$ between $10^{-37}\,\mathrm{cm^2}$ and $(2\text{–}3)\times10^{-31}\,\mathrm{cm^2}$ (the upper limit varies with m_χ), although the limit might change when re-calculated for a v^{-4} model (because the particles slow down as they scatter within the Earth). Therefore, experiments above the Earth's surface are more advantageous. A 1987 balloon experiment has ruled out $m_\chi > 2$–$3\,\mathrm{GeV}$ (the precise limit depends on uncertainties in the velocity distribution of the dark-matter halo)[62,63]. The rocket-based X-ray Quantum Calorimetry (XQC) experiment has excluded[64] $\sigma(200\,\mathrm{km\,s^{-1}}) > 1\times10^{-29}\,\mathrm{cm^2}$ for $m_\chi > 0.5\,\mathrm{GeV}$. The limits from all such experiments on lower dark-matter particle masses are quite weak, although this could change with new techniques[65,66].

A much stronger limit comes from the flip-side of the mentioned Earth interactions. The scattering of dark-matter particles within the Earth would heat it too strongly[67,68] unless $\sigma(200\,\mathrm{km\,s^{-1}}) < 10^{-32}(\mathrm{GeV}/m_\chi)\,\mathrm{cm^2}$, which is valid for m_χ values up to a few GeV; this implies that explaining the observed 21-cm signal at cosmic dawn requires $m_\chi < 5\,\mathrm{MeV}$. However, the Earth-heating constraint relies on some assumptions regarding dark-matter annihilation. Also, this and all the above direct detection limits on σ would be 3–4 orders of magnitude lower for spin-dependent interactions[62,68], whereas cosmic scattering with hydrogen would remain just as strong for such an interaction, given hydrogen's nuclear spin of $I = 1/2$ (note that ^{4}He would not contribute). In the case of a spin-dependent interaction, there might also be a direct effect of the dark-matter interaction on the spin temperature of hydrogen.

Because the collision energies in high-energy particle accelerators are typically orders of magnitude greater than 1 GeV, we assume that the relevant cross-section is σ_c. Accelerators may probe some of the parameter space that is relevant for 21-cm cosmology, but the limits depend strongly on the precise interaction type and nature of the dark-matter particle[66,69]. The proposed Search for Hidden Particles (SHiP) experiment at CERN has been motivated by the many possible physical mechanisms for producing very weakly interacting dark-matter particles in the MeV–GeV mass range[69]; cosmology may now provide additional impetus.

Astrophysical constraints on baryon–dark matter interactions are generally weaker than those we have considered here[67]. The most important limit, from cosmic rays, is often quoted as $\sigma(200\,\mathrm{km\,s^{-1}}) < 8\times10^{-27}[m_\chi/(1\,\mathrm{GeV})]\,\mathrm{cm^2}$, but this is valid only for large m_χ values (greater than about 100 GeV), and the limits on dark-matter particle masses in our range of interest are far weaker[70].

We again emphasize that we have assumed a v^{-4} dependence of the baryon–dark matter scattering cross-section, and any modification of this relation would have a major effect on the above comparisons of the cosmological signal with the various limits on baryon–dark matter interactions (as would other extensions of the parameter space, such as allowing only a fraction of the dark matter to scatter with baryons). Also, previous constraints have often been derived for a velocity-independent cross-section and must be carefully re-assessed for the case of a strong velocity dependence. The constraints on the dark-matter particle derived from the condition that it has the required relic cosmic density are model-dependent, as they depend on the annihilation cross-section (for thermal production) or the detailed production mechanism (for non-thermal production). If we assume an annihilation cross-section as expected for the weak interaction and a similar baryon–dark matter cross-section at relativistic velocities (so that $\sigma_c \approx 10^{-36}\,\mathrm{cm^{-2}}$), then the 21-cm signal suggests a dependence closer to v^{-3} than to v^{-4}.

Finally, we note that after this Letter was submitted, limits on baryon–dark matter scattering were derived[71] from low-redshift observations of the temperature of the intergalactic medium, based on the Lyman-α forest at $z \approx 5$. These limits are at relative velocities of about $10\,\mathrm{km\,s^{-1}}$, similar to the CMB limits discussed above. The derived upper limit of $\sigma_c = 3\times10^{-38}\,\mathrm{cm^2}$ for a v^{-4} model (for $m_\chi \ll 1\,\mathrm{GeV}$) is about five orders of magnitude greater than the minimum cross-section implied by the 21-cm signal at cosmic dawn, and it is stronger than the above CMB limit only for m_χ lower than about 1 MeV (although, as noted, the CMB limit must be carefully revised). Also, the low-redshift limit is uncertain because it depends on the history of photoheating of the intergalactic medium; the latter depends on the spatial and temporal distribution of the spectrum of ionizing sources, the distribution of Lyman-limit absorbers and the after-effects of inhomogeneous reionization, all of which are incompletely known. In the low-redshift probe, astrophysical heating is partly degenerate with baryon–dark matter interactions, and there is no unambiguous sign of dark matter similar to the excess absorption signal during cosmic dawn.

Code and data availability. We have opted not to make the code available because the calculations are based on the combination of published results on baryon–dark matter scattering[10] with our cosmic dawn numerical simulation code, the details and advantages of which have been described previously[15]. Confirmation of our basic results can be achieved by modifying other cosmic dawn codes, including publicly available ones[72]. The datasets generated or analysed in this study are available from the corresponding author on reasonable request.

31. Cohen, A., Fialkov, A., Barkana, R. & Lotem, M. Charting the parameter space of the global 21-cm signal. *Mon. Not. R. Astron. Soc.* **472,** 1915–1931 (2017).
32. Barkana, R. & Loeb, A. Detecting the earliest galaxies through two new sources of 21 centimeter fluctuations. *Astrophys. J.* **626,** 1–11 (2005).
33. Pritchard, J. R. & Furlanetto, S. 21-cm fluctuations from inhomogeneous X-ray heating before reionization. *Mon. Not. R. Astron. Soc.* **376,** 1680–1694 (2007).
34. Planck Collaboration. Planck 2015 results. XIII. Cosmological parameters. *Astron. Astrophys.* **594,** A13 (2016).
35. Ali-Haïmoud, Y. & Hirata, C. M. HyRec: a fast and highly accurate primordial hydrogen and helium recombination code. *Phys. Rev. D* **83,** 043513 (2011).
36. McQuinn, M. The evolution of the intergalactic medium. *Annu. Rev. Astron. Astrophys.* **54,** 313–362 (2016).
37. Miralda-Escudé, J., Haehnelt, M. & Rees, M. J. Reionization of the inhomogeneous Universe. *Astrophys. J.* **530,** 1–16 (2000).
38. Ross, H. E., Dixon, K. L., Iliev, I. T. & Mellema, G. Simulating the impact of X-ray heating during the cosmic dawn. *Mon. Not. R. Astron. Soc.* **468,** 3785–3797 (2017).
39. O'Leary, R. M. & McQuinn, M. The formation of the first cosmic structures and the physics of the $z \sim 20$ Universe. *Astrophys. J.* **760,** 4 (2012).
40. Semelin, B., Eames, E., Bolgar, F. & Caillat, M. 21SSD: a public data base of simulated 21-cm signals from the epoch of reionization. *Mon. Not. R. Astron. Soc.* **472,** 4508–4520 (2017).
41. Gnedin, N. Y. & Hui, L. Probing the Universe with the Lyα forest – I. Hydrodynamics of the low-density intergalactic medium. *Mon. Not. R. Astron. Soc.* **296,** 44–55 (1998).
42. Naoz, S. & Barkana, R. The formation and gas content of high-redshift galaxies and minihaloes. *Mon. Not. R. Astron. Soc.* **377,** 667–676 (2007).
43. Monsalve, R. A., Rogers, A. E. E., Bowman, J. D. & Mozdzen, T. J. Results from EDGES High-band. I. Constraints on phenomenological models for the global 21 cm signal. *Astrophys. J.* **847,** 64 (2017).
44. Ali, Z. S. *et al.* PAPER-64 constraints on reionization: the 21 cm power spectrum at $z = 8.4$. *Astrophys. J.* **809,** 61 (2015).
45. Patil, A. H. *et al.* Upper limits on the 21 cm epoch of reionization power spectrum from one night with LOFAR. *Astrophys. J.* **838,** 65 (2017).
46. Beardsley, A. P. *et al.* First season MWA EoR power spectrum results at redshift 7. *Astrophys. J.* **833,** 102 (2016).
47. Paciga, G. *et al.* A simulation-calibrated limit on the H I power spectrum from the GMRT Epoch of Reionization experiment. *Mon. Not. R. Astron. Soc.* **433,** 639–647 (2013).
48. Chuzhoy, L. & Shapiro, P. R. Ultraviolet pumping of hyperfine transitions in the light elements, with application to 21 cm hydrogen and 92 cm deuterium lines from the early universe. *Astrophys. J.* **651,** 1–7 (2006).
49. Chen, X. & Miralda-Escudé, J. The spin-kinetic temperature coupling and the heating rate due to Lyα scattering before reionization: predictions for 21 centimeter emission and absorption. *Astrophys. J.* **602,** 1–11 (2004).
50. Hirata, C. M. Wouthuysen–Field coupling strength and application to high-redshift 21-cm radiation. *Mon. Not. R. Astron. Soc.* **367,** 259–274 (2006).
51. Furlanetto, S. R. & Pritchard, J. R. The scattering of Lyman-series photons in the intergalactic medium. *Mon. Not. R. Astron. Soc.* **372,** 1093–1103 (2006).
52. Chuzhoy, L. & Shapiro, P. R. Heating and cooling of the early intergalactic medium by resonance photons. *Astrophys. J.* **655,** 843–846 (2007).
53. Hui, L., Ostriker, J. P., Tremaine, S. & Witten, E. Ultralight scalars as cosmological dark matter. *Phys. Rev. D* **95,** 043541 (2017).
54. Burns, J. O. *et al.* Probing the first stars and black holes in the early Universe with the Dark Ages Radio Explorer (DARE). *Adv. Space Res.* **49,** 433–450 (2012).
55. Ali-Haïmoud, Y., Chluba, J. & Kamionkowski, M. Constraints on dark matter interactions with standard model particles from cosmic microwave background spectral distortions. *Phys. Rev. Lett.* **115,** 071304 (2015).
56. Essig, R., Volansky, T. & Yu, T.-T. New constraints and prospects for sub-GeV dark matter scattering off electrons in xenon. *Phys. Rev. D* **96,** 043017 (2017).
57. Spergel, D. N. & Steinhardt, P. J. Observational evidence for self-interacting cold dark matter. *Phys. Rev. Lett.* **84,** 3760–3763 (2000).
58. Davidson, S., Hannestad, S. & Raffelt, G. Updated bounds on milli-charged particles. *J. High Energy Phys.* **5,** 3 (2000).
59. Dubovsky, S. L., Gorbunov, D. S. & Rubtsov, G. I. Narrowing the window for millicharged particles by CMB anisotropy. *J. Exp. Theor. Phys.* **79,** 1–5 (2004).
60. Read, J. I. The local dark matter density. *J. Phys. G* **41,** 063101 (2014).
61. Kadota, K., Sekiguchi, T. & Tashiro, H. A new constraint on millicharged dark matter from galaxy clusters. Preprint at https://arxiv.org/abs/1602.04009 (2016).
62. Zaharijas, G. & Farrar, G. R. Window in the dark matter exclusion limits. *Phys. Rev. D* **72,** 083502 (2005).
63. Rich, J., Rocchia, R. & Spiro, M. A search for strongly interacting dark matter. *Phys. Lett. B* **194,** 173–176 (1987).
64. Erickcek, A. L., Steinhardt, P. J., McCammon, D. & McGuire, P. C. Constraints on the interactions between dark matter and baryons from the x-ray quantum calorimetry experiment. *Phys. Rev. D* **76,** 042007 (2007).
65. Budnik, R., Chesnovsky, O., Slone, O. & Volansky, T. Direct detection of light dark matter and solar neutrinos via color center production in crystals. Preprint at https://arxiv.org/abs/1705.03016 (2017).

66. Battaglieri, M. *et al.* US cosmic visions: new ideas in dark matter 2017: community report. Preprint at https://arxiv.org/abs/1707.04591 (2017).
67. Starkman, G. D., Gould, A., Esmailzadeh, R. & Dimopoulos, S. Opening the window on strongly interacting dark matter. *Phys. Rev. D* **41,** 3594–3603 (1990).
68. Mack, G. D., Beacom, J. F. & Bertone, G. Towards closing the window on strongly interacting dark matter: far-reaching constraints from Earth's heat flow. *Phys. Rev. D* **76,** 043523 (2007).
69. Alekhin, S. *et al.* A facility to search for hidden particles at the CERN SPS: the SHiP physics case. *Rep. Prog. Phys.* **79,** 124201 (2016).
70. Cyburt, R. H., Fields, B. D., Pavlidou, V. & Wandelt, B. Constraining strong baryon-dark-matter interactions with primordial nucleosynthesis and cosmic rays. *Phys. Rev. D* **65,** 123503 (2002).
71. Muñoz, J. B. & Loeb, A. Constraints on dark-matter-baryon scattering from the temperature evolution of the intergalactic medium. *J. Cosmol. Astropart. Phys.* **2017,** 043 (2017).
72. Mesinger, A., Furlanetto, S. & Cen, R. 21CMFAST: a fast, seminumerical simulation of the high-redshift 21-cm signal. *Mon. Not. R. Astron. Soc.* **411,** 955–972 (2011).